Copyright @ by Tanta University, Egypt

Delta J. Sci. 2010, 34: 25- 42 GEOLOGY

Chemistry And Mineral Chemistry Of Zircon In Alkaline Granites, South Sinai, Egypt.

H. M. Sherif*; R. Bousquet **; M. M. Gabr* and M. S. Azab*

*Nuclear Materials Authority, Cairo,Egypt. P.O. Box 530
** Institute fuer Geowissenschaften, Karl-Liebknecht-Str. Potsdam-Golm, Germany.

(Received: 20-12-2009)

ABSTRACT: Such geochemical investigations of alkaline granites as both Wadi Sieh and Wadi Lethi, south Sinai, Egypt, indicate that they are A-type granites. They are similar in major and trace elements but differ in rare earth elements (REE). The alkaline granite of Wadi Sieh (AGS) is enriched in LREE whereas the alkaline granite of Wadi Lethi (AGL) is enriched by MREE and HREE.

Zircon crystals on both AGS and AGL are studied using Scanning Electron Microscopy (SEM) and analyzed for major, trace and rare earth elements by electron microprobe in order to reveal the relation between whole-rock chemistry and zircon morphology and chemistry.

The faces of zircons on both AGS and AGL are affected by alkaline magma during their crystallization period reflecting a development of {101} pyramidal faces. This study indicates that no relation is noticed between trace elements of zircon and whole-rock chemistry while, ∑REEs of zircon increases with increasing of phosphorus not with the ∑REE of whole-rock.

INTRODUCTION: Zircon, $ZrSiO_4$, is a mineral of singular importance in earth science where it has become one of the most widely used minerals for the extraction of information on the prehistory and genesis of magmatic, metamorphic and sedimentary rocks. Much of the geological usefulness of zircon stems from its suitability as a geochronometer based on the decay of (U and Th) to Pb. Natural zircon crystals commonly contain trace amounts of REE, Y, P, Hf, U, and Th, although some zircon crystals contain several weight percent of these elements (Speer 1982) and are enriched in heavy rare-earth elements (HREE) to be compared with (LREE) and middle rare-earth elements (MREE). This enrichment in HREE has been reported for synthetic zircon crystals (Watson 1980; Fujimaki 1986), as well as for natural samples (e.g., Nagasawa 1970; Gromet and Silver 1983; Heaman et al. 1990; Hinton and Upton 1991; Paterson et al. 1992; Barbey et al. 1995; Bea 1996; Schaltegger et al. 1999). Many zircon crystals have high P (Phosphorus) concentrations, leading some authors to propose a solid solution between zircon and xenotime (YPO_4), which is isostructural with zircon (Wopenka et al. 1996; Belousova et al. 1998).

Zircon can also provide compelling chemical evidence for the mineral–melt–fluid processes operating during crust formation and maturation, hydrothermal alteration and diagenesis (Hanchar and van Westrenen 2007; Harley et al. 2007; Geisler et al. 2007). Since most cations in zircon have very low diffusivity, many of zircon's chemical signatures are preserved either from the time of its formation or from the later significant geological process to have acted on and modified its chemistry (Cherniak and Watson 2002).The relation between zircon saturation, crystallization and melt composition was investigated by Watson (1979) and revisited by Watson and Harrison (1983). The experimental saturation relation is most commonly used for the calculation of zircon saturation temperatures for natural rocks, which are used to assess whether or not zircon was an early or late crystallizing phase. Dickinson and Hess (1982) experimentally determined that early zircon saturation (at 1100°C) in Lunar granites would require the granites to have a whole-rock Zr abundance of 5000 ppm and late-stage Lunar basalts to have 9000 ppm Zr given that these Lunar rocks have Zr abundances of about 200-1800 ppm, zircon would have saturated at ~1100°C after >99.9% whole-

rock crystallization. This precludes zircon crystallization as a significant influence on the trace-element evolution of lunar magmas.

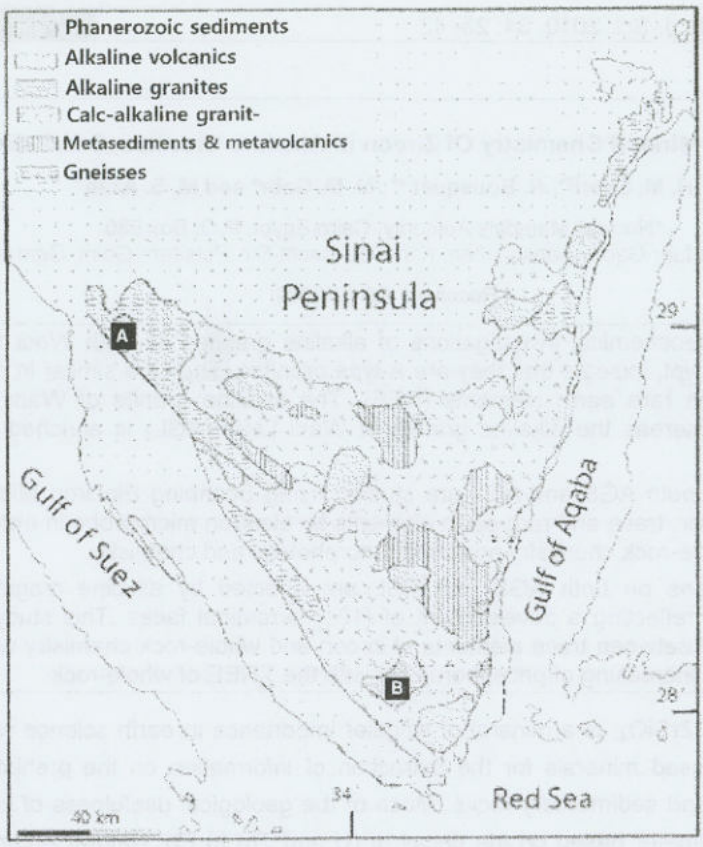

Fig. 1. Simplified geological map of Sinai, Egypt (after Shimron, 1980) showing locations of the studied areas. **A** = Wadi Sieh **B** = Wadi Lethi

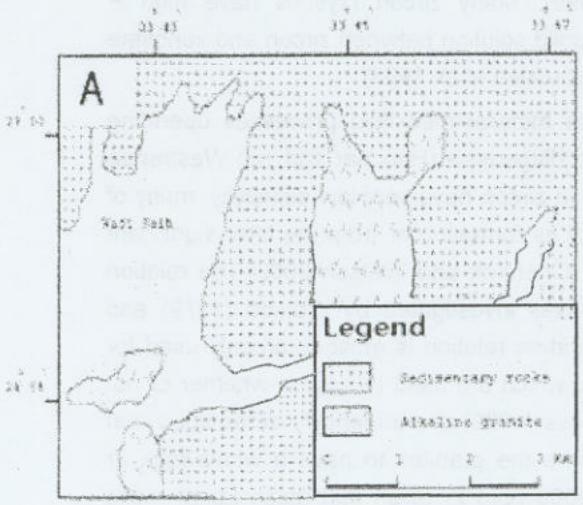

Fig. 2A. Simplified geological map of Wadi Sieh area (after Gabr 2005).

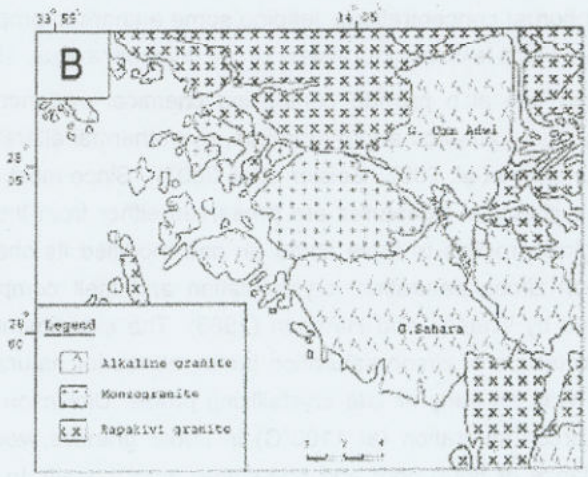

Fig. 2B. Simplified geological map of Wadi Lethi area (after Mosalhi 2006).

Moreover, zircon has a highly variable external morphology. Often crystals are faceted with combinations of prism ({100} and {110}) and pyramid forms ({211}, {101} and {301}). Since the 1950s there have been attempts to systematically relate zircon morphology to petrogenesis (Poldervaart 1955, 1956; Larsen and Poldervaart 1957, Pupin and Turco 1972a,b,c; Kostov 1973, Hoffmann 1981). A typologic scheme relating the relative development of crystal forms with temperature and host-rock type was published by Pupin (1980).

The main target of the present study is to compare between the morphology and chemistry of zircon and their host alkaline granite to illustrate the effects of the alkaline magma on the morphology and chemistry of zircon.

Geologic setting

The selected studied alkaline granities occur in two areas; Wadi Sieh and Wadi Lethi, south Sinai, Egypt (Fig.1).

Wadi Sieh alkaline granite (AGS) occurs as small scattered hilly exposures outcropping at Wadi Seih (Fig. 2 A). It is considered to be a member of the alkaline series in south Sinai (Gabr 2005) and have low relief with coarse grains and rosy colour. They are highly jointed with red hematitic impregnations along the joint plains.

The alkaline granitic rocks exposed at Wadi Lethi (AGL) (Fig. 2B) contain riebeckite and cropping out over an area of 55 km^2 as elongated masses in the upstream section of Wadi Lethi. They cut by dyke swarms varying in composition from mafic to felsic and trending in NE-SW and NW-SE directions (Mosalhi, 2006).

Analytical techniques

Whole-rock geochemistry

Sixteen representative fresh rock samples from AGS and AGL are selected for whole-rock geochemical analysis. Major elements were done by X-ray fluorescences (XRF) using Philips PW 1450 automatic spectrometer on fused discs in the laboratories of Nuclear Materials Authority, Cairo, Egypt. Sixteen samples were analyzed for trace and twelve for rare earth elements using inductively coupled plasma mass spectrometry (ICP-MS) at ACME Analytical Laboratories, LTD., Vancouver, Canada.

Scanning Electron Microscopy (SEM)

Ten samples of fresh rock were crushed and extracted using common techniques such as heavy liquids and Frantz isodynamic magnetic separator at Nuclear Materials Authority, Egypt. Backscattered-electron (BSE) images were taken using A Philips (XL30) ESEM, equipped with an energy dispersive X-ray spectrometer at Nuclear Materials Authority, Egypt.

Microprobe

Twenty of electron microprobe zircon analyses using model CAMECA SX50 were carried out in the Institute of Wissenschaftspork Albert Einstein, Potsdam University, Germany.

Table 1. Major oxides analyses (Wt %), norm values, trace elements (ppm) of the studied Wadi Lethi alkaline granite (AGL).

Sample.	43	33	45	8	94	28	D-7	D-8	Av.
Major oxides (Wt %)									
SiO_2	75.80	76.28	76.09	75.55	75.05	76.1	75.6	74.8	75.67
TiO_2	0.13	0.18	0.17	0.73	0.4	0.11	0.19	0.23	0.27
Al_2O_3	11.23	10.04	10.98	11.15	10.84	11.59	10.94	11.32	11.01
Fe_2O_3	1.0	0.44	1.3	1.28	1.47	1.00	1.04	1.33	1.11
FeO	1.6	1.6	1.23	0.43	0.84	0.99	0.78	0.58	1.01
MgO	0.05	0.03	0.07	0.10	0.02	0.08	0.09	0.04	0.06
CaO	0.24	0.29	0.28	0.12	0.28	0.19	0.3	0.25	0.24
Na_2O	4.45	5.8	4.59	4.15	4.15	4.7	5.73	5.78	4.92
K_2O	4.45	5.45	4.55	5.58	5.3	4.89	5.42	5.40	5.13
P_2O_5	0.02	0.02	0.023	0.02	0.02	0.02	0.05	0.07	0.03
L.O.I	0.25	0.26	0.4	0.45	0.45	0.33	0.25	0.3	0.34
Total	99.22	100.39	99.683	99.56	98.82	100	100.39	100.1	99.77
CIPW norm									
Q	52.32	47.71	51.86	48.54	49.18	50.83	47.16	46.57	49.27
Or	26.6	32.19	27.11	33.3	31.87	29.02	32.01	32	30.51
Ab	0	0	0	0	0	0	0	0	0
An	0	0	0	0	0	0	0	0	0
C	0	0	0	0	0	0	0	0	0
Ac	2.92	1.27	3.78	3.73	4.31	2.9	3	3.85	3.22
Ns	8.08	11.06	8.1	7.25	7.16	8.51	10.47	10.38	8.88
Di	0.45	0.55	0.53	0.2	0.54	0.35	0.5	0.35	0.43
Di	0.02	0.02	0.05	0.05	0.03	0.04	0.09	0.05	0.044
Di	0.49	0.6	0.54	0.16	0.57	0.34	0.45	0.33	0.44
Hy	0.1	0.06	0.13	0.2	0.02	0.16	0.13	0.05	0.11
Hy	2.26	2.03	1.45	0.63	0.32	1.3	0.67	0.35	1.13
Mt	0	0	0	0	0	0	0	0	0
He	0	0	0	0	0	0	0	0	0
Il	0.25	0.34	0.33	0	0.77	0.21	0.36	0.44	0.34
Ap	0.04	0.04	0.05	0.04	0.04	0.04	0.11	0.15	0.06
Trace elements (ppm)									
Cr	7	11	13	18	17	9	15	14	13
Co	6	5	5	7	7	3	7	8	6
Ni	8	8	6	6	5	4	8	8	6.625
Cu	11	13	20	12	11	11	12	15	13.12
Zn	134	102	101	124	105	47	154	120	110.9
Zr	796	480	484	661	843	150	755	450	577.4
Rb	145	140	146	95	150	113	124	140	131.6
Y	58	35	39	43	67	35	53	45	46.88
Hf	18	13	18	14	19	11	19	13	15.63
Ba	326	229	239	374	135	337	365	235	280
Pb	39	22	22	15	28	13	25	22	23.25
Sr	25	73	33	59	57	65	86	75	59.12
Ga	37	21	18	26	29	14	28	23	24.5
V	4	4	6	3	10	7	6	4	5.5
Nb	85	53	75	95	81	74	75	80	77.25
Th	6	8	6	5	8	4	14	7	7.25
U	15	17	13	15	18	13	35	16	17.75

Table 2. Major oxides (wt %),CIPW norm and trace elements (ppm) analyses for the studied Wadi Seih alkaline granites (AGS)

Major oxides (Wt %)									
Sa.No.	**1**	**2**	**3**	**4**	**5**	**6**	**7**	**8**	Av
SiO_2	74	77	75.88	74.02	75.3	74.6	75.12	74.28	75.02
TiO_2	0.22	0.21	0.2	0.21	0.23	0.24	0.23	0.24	0.22
Al_2O_3	11	8.7	9.3	10.8	8.7	9.4	9.4	10.7	9.75
Fe_2O_3	2.9	2.1	2.8	2.7	3.56	3.8	3.1	3.2	3.02
MnO	0.02	0.06	0.07	0.08	0.06	0.02	0.03	0.024	0.04
MgO	0.53	0.3	0.31	0.52	0.51	0.75	0.31	0.51	0.46
CaO	0.6	0.53	0.7	0.7	0.64	0.7	0.47	0.71	0.63
Na_2O	4.2	4.99	4.8	4.5	4.99	4.24	4.98	4.38	4.64
K_2O	5.2	5.21	5.12	5.1	5.11	5.02	5.4	5.04	5.15
P_2O_5	0.04	0.08	0.05	0.06	0.04	0.06	0.04	0.08	0.052
L.O.I	0.7	0.6	0.65	0.7	0.62	0.63	0.53	0.43	0.61
Total	99.41	99.78	99.88	99.39	99.76	99.46	99.61	99.594	99.61
CIPW norm									
Q	45.95	49.29	47.8	46.18	45.84	45.72	45.61	46.08	46.56
Or	31.16	31.07	30.52	30.57	30.49	30.04	32.24	30.06	30.77
Ab	0	0	0	0	0	0	0	0	0
An	0	0	0	0	0	0	0	0	0
C	0	0	0	0	0	0	0	0	0
Ac	8.48	6.11	8.15	7.9	10.37	11.1	9.03	9.32	8.81
Ns	6.13	8.29	7.37	6.89	7.17	5.51	7.5	6.23	6.89
Di	1.16	0.91	1.02	1.32	1.24	1.32	0.88	1.29	1.14
Di	0.98	0.7	0.78	1.05	1	1.12	0.72	1.08	0.93
Di	0.03	0.1	0.13	0.12	0.09	0.02	0.05	0.04	0.07
Hy	0.36	0.05	0	0.27	0.28	0.78	0.06	0.21	0.25
Hy	0.01	0.01	0	0.03	0.02	0.02	0	0.01	0.012
Ol	0	0	0	0	0	0	0	0	0
Ol	0	0	0	0	0	0	0	0	0
Mt	0	0	0	0	0	0	0	0	0
He	0	0	0	0	0	0	0	0	0
IL	0	0	0	0	0	0	0	0	0
Ap	0.09	0.18	0.11	0.13	0.09	0.13	0.09	0.18	0.125
Trace elements (ppm)									
Cr									
Co	1.4	2.6	1	1	2	1.5	1.4	1.5	1.55
Ni	43.1	34.3	47	71	26.5	41.5	45.1	44	44.06
Cu	10.8	19.6	5.9	9	3.8	3	18.1	10	10.03
Zn	133	109	227	62	110	122	24	112	112.38
Zr	280.3	322.5	464.4	420	315.2	371.9	350.4	360.6	360.66
Rb	155.5	156.6	164.4	162	143	139	125	149.3	149.35
Y	99.1	118.3	139.3	103.8	86.6	96.9	91.9	105.1	105.13
Hf	10.1	11.8	14.8	14	9.7	11.8	11.6	12	11.975
Ba	42.6	205.9	62.3	112	82.3	123.2	191.9	117.1	117.16
Pb	155.5	156.6	164.4	162	143	139	125	149.3	149.35
Sr	13.3	11.5	8.7	10.4	11.7	8.9	45.5	15.7	15.71
Ga	31.3	31	31.9	30.4	27.6	28.4	29.3	30	29.98
V							8	7	7.5
Nb	33.1	38.2	45.7	38.4	31.4	36	46.2	38.4	38.43
Th	12.7	14.2	13.8	13.9	10.9	11.5	12.4	13.4	12.85
U	9.8	10.5	6.4	5.8	4.3	4.2	5.9	6.5	6.68

Results and discussion

The chemical analyses for the major oxides as well as the trace and rare earth elements of the studied alkaline granites from AGS and AGL are presented in Tables (1, 2 and 3).

In order to observe the differences between the elemental constituents of AGL and AGS and facilitate the comparison between them, the averages of their major oxides, trace and rare-earth elements listed on tables 1,2 and 3 are graphically representative (Fig.3 A, B&C). The figure shows that the two rock units have a relatively an equal SiO_2, TiO_2, P_2O_5, K_2O and Zn contents. The former has high FeO and Na_2O relative to the later while the later has high contents of Fe_2O_3, MgO and CaO if compared with the former (Fig.3 A). This may ascribe to the presence of a relatively high sodic plagioclase percentage in the AGL and the occurrence of much more biotite and apatite in the AGS compared with the AGL one. The average of Cr, Co, Zr, Ba, Sr and Nb in the AGL is higher than those present in the AGS one while the averages of Ni, Rb, Y, Pb, Ga and V are higher in case of the AGS (Fig.3 B). Figure 3C shows that the AGS has high LREEs compared with the AGL which has high percentage of the MREE and HREEs. This may suggest the presence of some accessory minerals such as zircon and monazite in the AGS. The pattern of AGS shows slope from LREE to HREE (Fig 3) and enriched in LREE, while the pattern of AGL shows enrichment in MREE and HREE (Fig. 3C).

The Chemical data of the studied AGL and AGS are plotted on the multi-cationic R1-R2 [4Si - 11(Na+K) - 2(Fe+Ti) - 6Ca + 2Mg + Al] diagram of De La Roche et al. (1980) where their data points fall within the alkali granite field (Fig. 4).

The Zr+Y+Nb+Ce versus Fe_2O_3/MgO diagram was used by Whalen et al.(1987) to distinguish A-type granites (alkaline, anorogenic) fractionated felsic I-type granites (FG) and unfractionated M, I- and S-type granites (OGT, orogenic). The authors (op.cit) considered that a part of A-type granites belong to the highly fractionated I-type granites. Figure (5) shows such distinction where all the studied alkaline granite samples fall within the A-type field of Whalen et al.(op.cit.). The A-type granites are further subdivided into two chemical groups according to their Y/Nb-Rb/Nb ratios (Eby, 1992); 1) group A1 has a Y/Nb < 1.2 represents anorogeneic rifting environment and 2) group A2 has Y/Nb > 1.2 and comprise post-collision and post-orogenic suits of island-arcs and continental margins. On the Nb -Y- Ce diagram of Eby (1992), it is observed that the AGL plot within the A1 group field and consequently correspond to the anorogenic rifting environment (Fig.6). Also, the AGS fall in the A2 group field and pertain to post-orogenic setting.

The tectonic setting of the granitoid rocks is discussed by Pearce et al (1984) who used the relation between Y and Nb to separate between the WPG and VAG + Syn-COLG. Figure (7) shows such relation where the studied samples of both AGL and AGS lie within the WPG field.

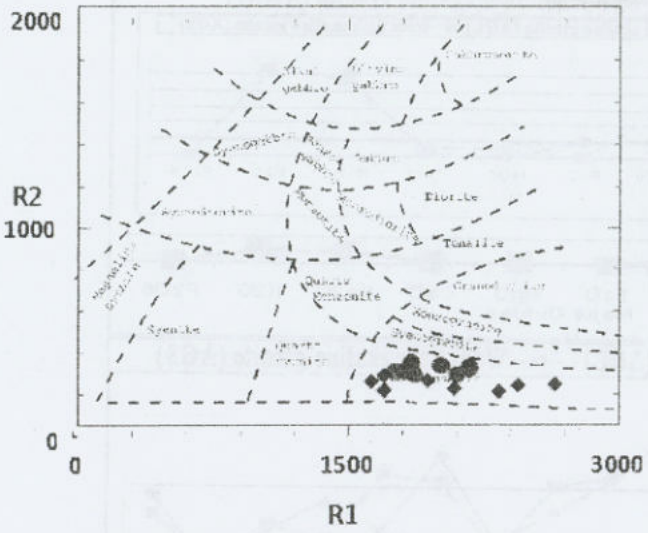

Fig. 4. R1-R2 multicationic diagram (De La Roche et al., 1980) showing classification of studied granites .= AGS ● = AGL ◆

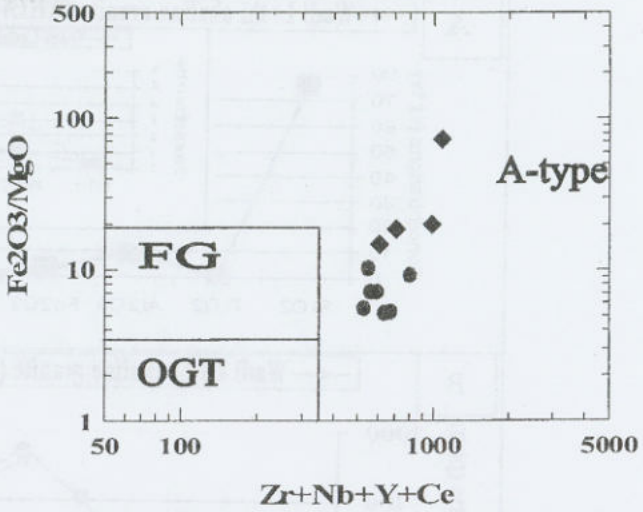

Fig.(5):Zr+Y+Nb+Ce versus Fe_2O_3/MgO of A-type granites; fractionated felsic I-type granites (FG) and unfractionated M, I- and S-type granites (OGT, orogenic). Whalen et al.(1987). Symbol as in Fig.4.

Table 3. Rare earth elements analyses for the studied alkaline granites.

S. No.	La	Ce	Pr	Nd	Sm	Eu	Gd	Tb	Dy	Ho	Er	Tm	Yb	Lu	∑REE
Wadi Seih alkaline granites (AGS).															
1	55.8	125	16.2	64.9	16.1	0.31	16.51	2.75	16.33	3.33	9.18	1.3	7.92	1.14	336.77
2	58.1	127.6	17.4	71.5	18.1	0.21	19.26	3.29	19.61	3.97	11.39	1.51	9.59	1.34	362.87
3	71.1	163.8	21.86	88.2	23.5	0.28	23.17	3.9	22.91	4.65	12.94	1.79	11.34	1.55	450.99
4	48.8	126	15.21	63.3	16.1	0.23	16.43	2.89	17.61	3.7	10.73	1.52	9.8	1.32	333.64
5	55	134	16.52	65.7	16.5	0.24	15.59	2.63	15.18	2.97	8.71	1.2	7.3	1.04	342.58
6	62.1	138.9	18.3	75	18	0.27	17.57	2.93	17.43	3.47	9.63	1.33	8.12	1.12	374.17
7	41	68.7	13.64	52.8	12.4	0.28	11.78	2.38	15.2	3.3	9.26	1.27	8.14	1.07	241.22
Av.	55.99	126.3	17.0	68.8	17.2	0.26	17.19	2.97	17.75	3.63	10.26	1.42	8.89	1.23	348.89
Wadi Lethi alkaline granites (AGL).															
1	9.8	39.3	5.37	24.1	9.22	0.6	10.05	2.38	15.2	3.18	10.08	1.77	10.79	1.49	143.36
2	11.9	40.2	7.8	30.5	11.2	2.95	33.3	6.4	23.9	5.78	34.5	2.8	11.3	3.57	226.1
3	18.6	111.1	19.44	71.7	43.3	0.56	21.88	11.9	61.7	11.4	31.02	4.59	28.69	3.58	439.41
4	14.9	62.4	6.21	28.6	10.1	1.01	12.89	4.3	29.4	7.43	31.4	9.33	22.78	17.6	258.35
5	66.5	89.8	12.44	63.4	22.8	5.34	85.48	18.5	89.9	16.9	47.57	10.7	78.88	11.9	619.97
Av.	24.34	68.56	10.25	43.7	19.3	2.09	32.72	8.68	44.0	8.94	30.91	5.84	30.49	7.61	337.44

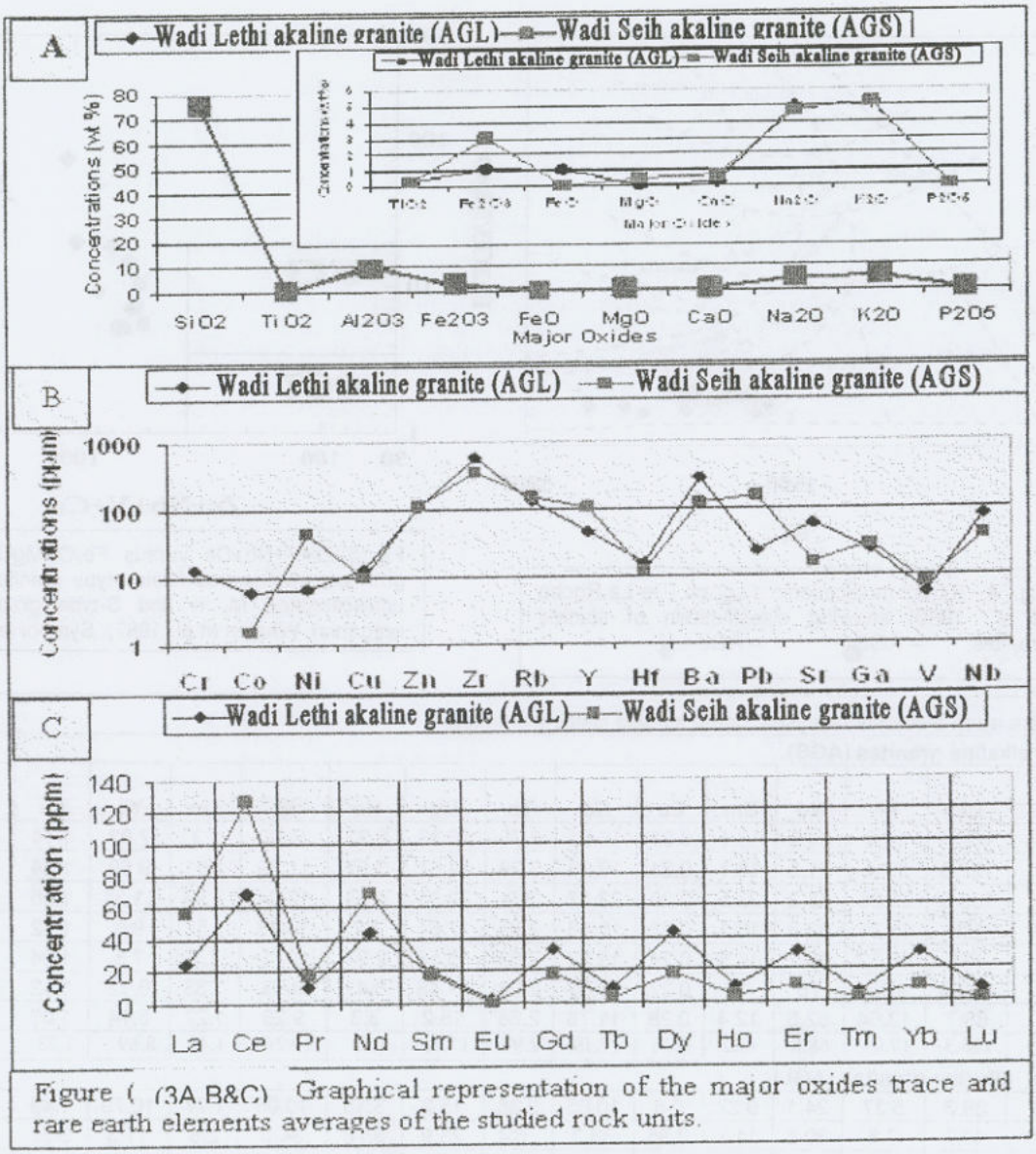

Figure ((3A,B&C) Graphical representation of the major oxides trace and rare earth elements averages of the studied rock units.

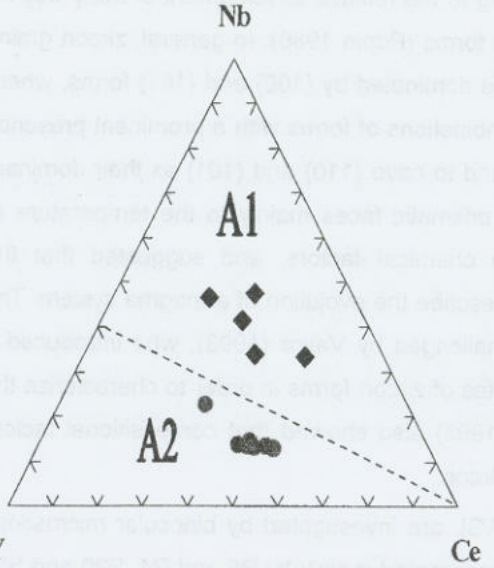

Fig.(6):Nb–Y–Ce discriminant diagram for the subdivision of A-type granites (after Eby, 1992). Symbols as in Fig.4.

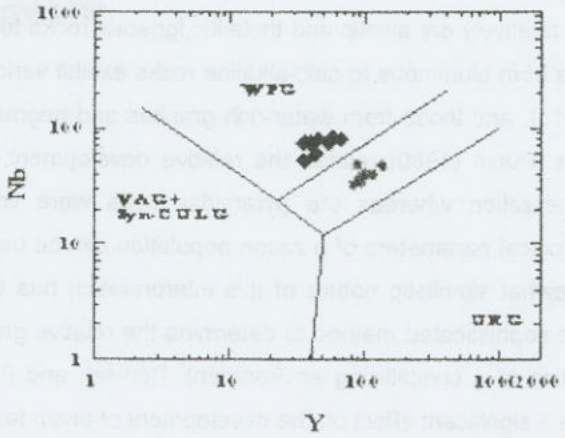

Fig.7. Y-Nb tectonic setting discrimination diagram of the studied granitoids (After Pearce et al.1984). Symbols as in Fig. 4

Condie(1973) used the relation between Rb and Sr to deduce the crustal thickness during the placement of the granitoids. Figure (8) shows that the AGL has been emplaced at depth ranging between 20-30 Km whereas the AGS has been emplaced at depth less than 20 Km. Accordingly, the AGL has been emplaced at relatively deeper depth while the AGS has been emplaced at shallow level.

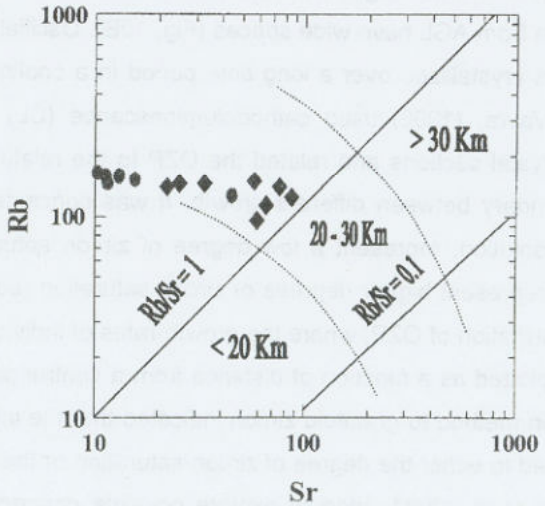

Figure (8): Rb-Sr variation diagram for the studied granitoids. Condie, 1973). Symbols as Fig. 26.

Morphology of zircon

Systematic examination of zircon typology has led to the establishment of the widely used "Pupin diagram",(Fig.9) in which zircon crystals are classified according to the relative development of the {100} vs. {110} prismatic forms and the {211} vs. {101} pyramidal crystal forms (Pupin 1980). In general, zircon grains from relatively dry alkalic and tholeiitic igneous rocks tend to be dominated by {100} and {101} forms, where those from aluminous to calc-alkaline rocks exhibit various combinations of forms with a prominent presence of {211}, and those from water-rich granites and pegmatites tend to have {110} and {101} as their dominant forms. Pupin (1980) related the relative development of the prismatic faces mainly to the temperature of crystallization whereas the pyramidal faces were linked to chemical factors, and suggested that the typological parameters of a zircon population can be used to describe the evolution of a magma system. The somewhat simplistic nature of this interpretation has been challenged by Vavra (1993), who introduced a more sophisticated method to determine the relative growth-rates of zircon forms in order to characterize the kinetics of a crystallizing environment. Benisek and Finger (1993) also showed that compositional factors have a significant effect on the development of prism faces in zircon.

The morphology of the studied zircons of both AGS and AGL are investigated by binocular microscope and SEM image. Zircons of alkaline granites from AGS are represented mainly by P5 and P4, S20 and S25 are less abundant, and P3, S15 and P2 occur only in minor amounts, (Fig. 8A) whereas zircons of AGL are represented by P4, P5 and S 25 but P3 and P2 occur in minor amounts (Fig, 8B). Also, BSE shows that {100} prismatic forms and {101} pyramidal forms are the dominant in the studied zircons whether from AGS or AGL (Fig. 9A and B).

Thus, it is clear that morphology of zircon is affected by the composition and possibly the temperature of the crystallization medium.

Zircon from both AGS and AGL show oscillatory zoning (Fig. 10A and B). Figure 10A shows oscillatory zoning of zircon from AGS, the pattern include bright and dark zones. Both dark and bright zones have narrow spaces but the zones in zircon from AGL have wide spaces (Fig. 10B). Oscillatory zoning of zircon is considered as evidence that zircon is crystallized over a long time period in a cooling magma (e.g., Silver and Deutsch 1963, Kohler 1970). Vavra, (1990) used cathodoluminescence (CL) images of oscillatory zoning patterns (OZP) of oriented crystal sections and related the OZP to the relative growth velocities of crystal faces by delineating the boundary between different growth. It was concluded that widely spaced OZP, interrupted by surfaces of dissolution, represent a low degree of zircon saturation in the melt and narrowly-spaced uninterrupted OZP represent higher degrees of zircon saturation (super saturation). Vavra (1993) quantified the growth-rate information of OZP, where the growth-rates of individual crystal faces were normalized to a reference face and plotted as a function of distance from a central point (representing zero time). Application of this quantification method to granitoid zircon indicated that the influence on the growth-rate of different forms can be attributed to either the degree of zircon-saturation or the incorporation of trace-elements (Vavra 1994). Also, Poller et al. (2001) tried to explore possible connections between the CL emission of natural zircon crystals and their chemical composition. The author (op.cit) found that neither the REE nor trace elements such as Y or Th were found to have any direct correlation with the CL brightness and also the intensity of the CL signals was not directly reflected in the REE concentrations or the shape of the REE patterns but uranium is probably the element responsible for quenching or suppressing the CL

signals. Benisek and Finger (1993), in a combined BSE imaging and electron microprobe study, reported the enrichment of U, Hf, and Y in BSE bright zones, which are usually equivalent to dark zones in CL. Similar results were published by Hanchar and Miller (1993), who found an inverse relationship between the CL emission from zircon and its U and Hf content.

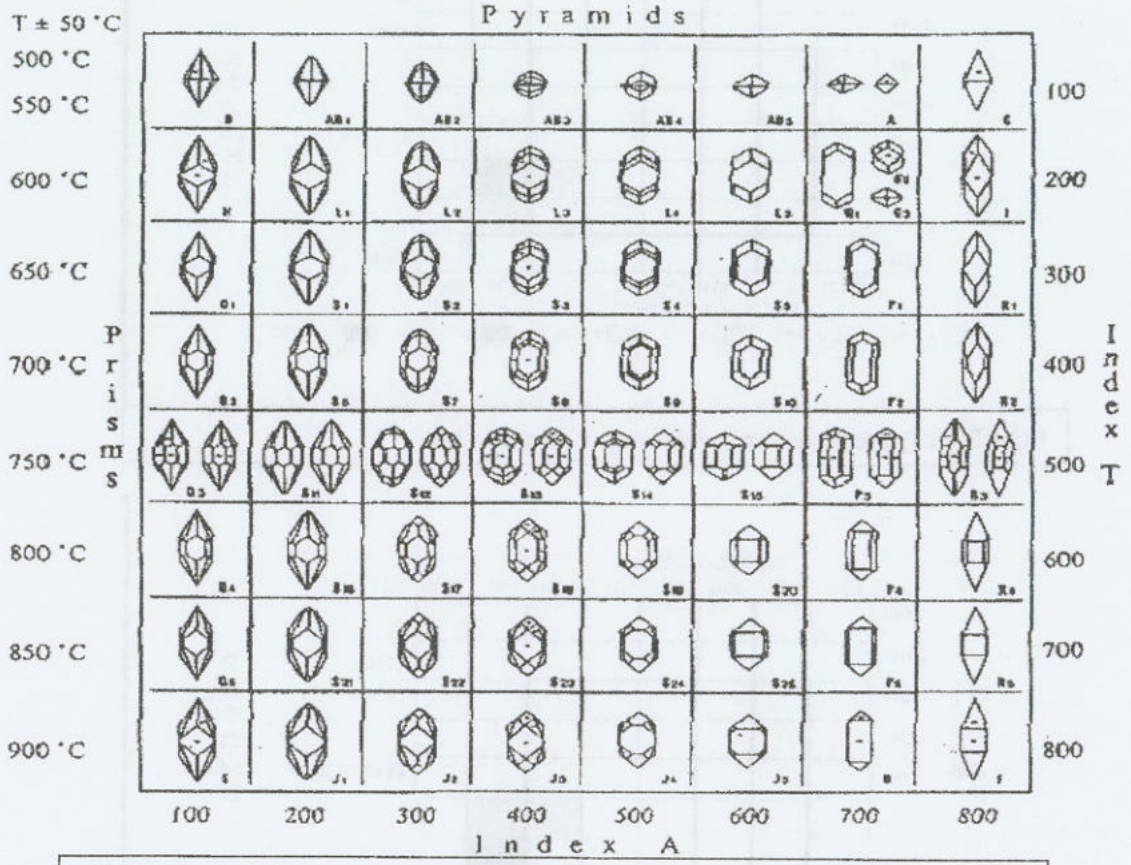

Fig.(9): Typologic diagram of natural abundances of zircon types, (Pupin, 1980).

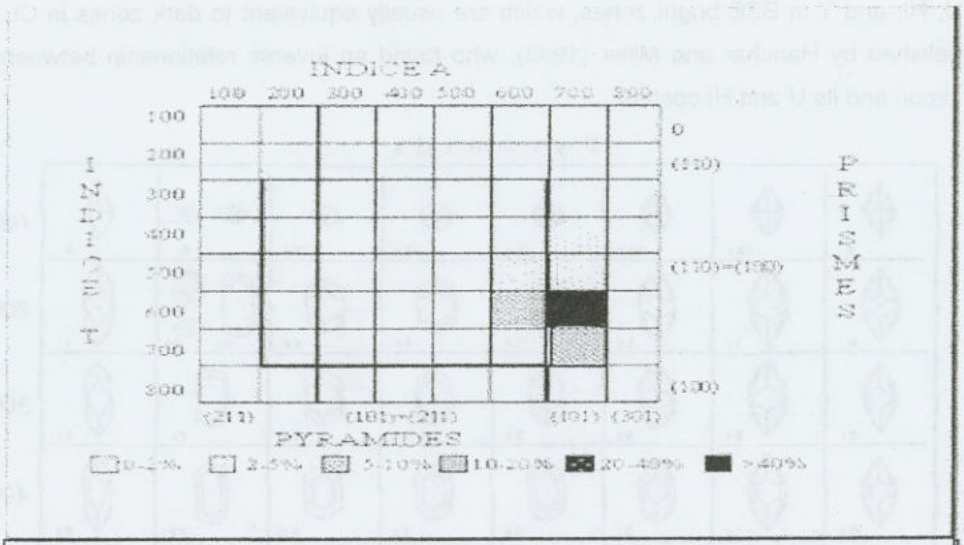

Fig.(8B): Typologic frequency distribution of zircons on AGL

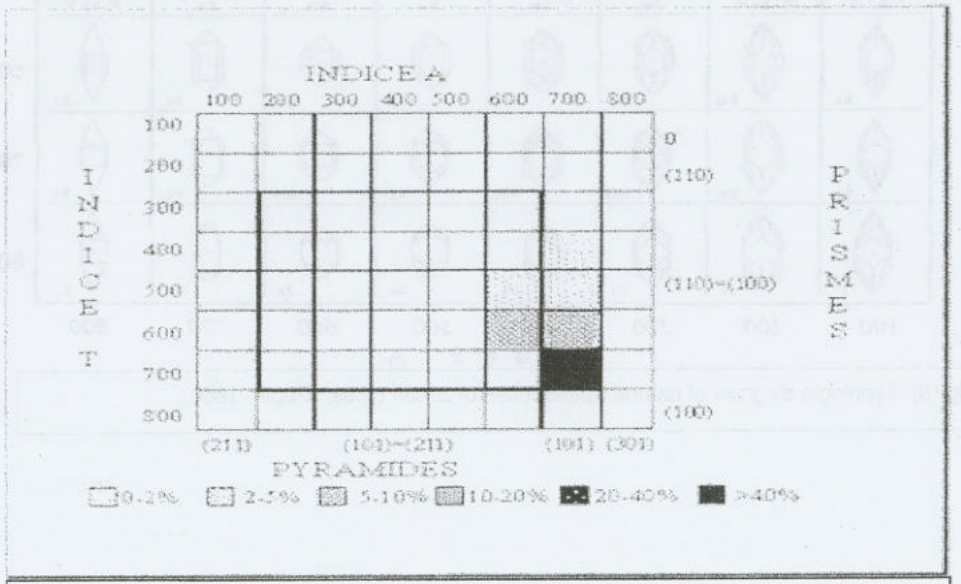

Fig. (8A): Typologic frequency distribution of zircons on AGS

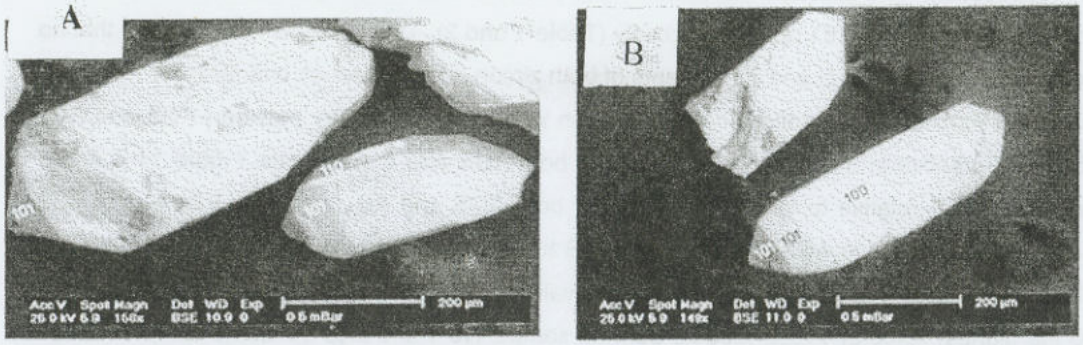

Fig (9): BSE shows prismatic {110} and pyramidal {101} faces for the studied zircons
A= zircon of AGS B = zircon from AGL

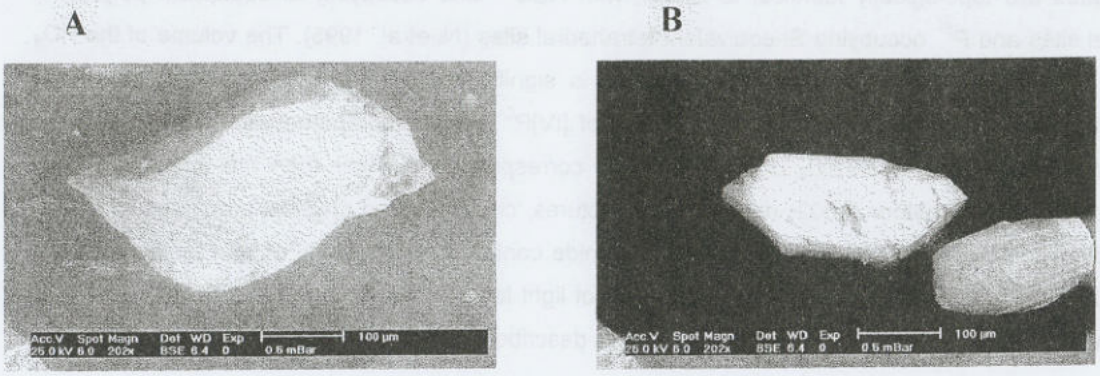

Fig.(10): BSE shows zoning in the studied zircon. A= zircon of AGS B = zircon of AGL

Results of electron microprobe analyses of zircon from AGS and AGL are listed in Tables 4 and 5. The averages of ZrO_2, SiO_2 and HfO_2 of zircon from AGS are 64.82, 32.13 and 1.53 wt %, respectively whereas the reported averages of those oxides for zircons from AGL are 64.56, 32.2 and 1.21 wt % respectively. The most important major oxide is HfO_2 whereas hafnon mineral exhibits extensive solid solution with zircon, and only hafnon ($HfSiO_4$) and zircon have complete solid-solution (Ramakrishnan et al. 1969, Hoskin and Rodgers 1996). The extent of this solid solution in natural zircon is typically restricted although variation of the Zr/Hf ratio in zircon away from the chondritic value of ~37 is common. Several attempts have been made to use HfO_2 value as indicator for host rocks, for example: meteoritic zircon, 1.08-1.45% (Ireland and Wlotzka 1992); lunar zircon, 1.18% average (Wopenka et al. 1996); carbonatite zircon, Finland, 0.98% (Halden et al. 1993); diorite, China, ~1-3% (Wang et al. 2002) and from Chile, up to 1.65% (Ballard et al. 2002); granodiorite zircon, Chile, as low as 0.15% (Ballard et al. 2002); granite zircon, California, 1.78-3.17% (Wark and Miller 1993) and from the Czech Republic, up to 12.3% (Uher et al. 1998). It is obvious that no distinctive limits between HfO_2 values for different rocks. The wide ranges render overlaps between HfO_2 values from different rocks hence, it appears that the HfO_2 values increases with magmatic differentiation and not with the magma type (Sawka 1988). The average U and Th contents of zircon from AGS are 687.5

and 316.4 ppm respectively, while the averages of the two radioelements reported for AGL are 387.8 ppm and 210.9 ppm, respectively. The average contents of whole-rock U and Th of AGS and AGL are 6.6 ppm and 12.59 ppm; and 6.5ppm and 23.61 ppm respectively (Table 1 and 2). These values may suggest that no direct correlation exists between the U and Th contents of both zircon and whole-rock chemistry.

An expectation of zircon chemistry reflects the different in whole rock chemistry between AGS and AGL since no significant differences in the patterns of REE from both AGS and AGL zircons. Figure 11 A and B shows enrichment in HREE relative to LREE for zircons of both AGS and AGL while the whole rock REE chemistry are different from AGS to AGL. Zircons from AGS have the highest value of ∑REE (4451.8 ppm) in sample N0 3 and also the same sample has the highest value for P (161.5 ppm), (Table 4), while zircons from AGL have the highest value of ∑REE (2698.5 ppm) in sample No 4 and also the same sample has the highest value of P (144.0 ppm), (Table 5). So, the ∑REE of both AGS and AGL can be correlated with P. Speer (1982) discussed the correlation between REE and P in substitution of zircon and he proposed the following equation: $[(Y,REE)^{3+} + P^{5+} = Zr^{4+} + Si^{4+}]$ to discuss the substitution of REE in zircon crystal which, called (xenotime substitution mechanism). The structures of xenotime and the other zircon-group orthophosphates are topologically identical to zircon, with REE^{3+} ions occupying Zr-equivalent polyhedral dodecahedral sites and P^{5+} occupying Si-equivalent tetrahedral sites (Ni et al. 1995). The volume of the PO_4 tetrahedron in xenotime-type $REEPO_4$ orthophosphates is significantly smaller than the analogous SiO_4 tetrahedron in zircon, reflecting the smaller ionic radius of $[IV]P^{5+}$ (0.15Å) compared with [IV]Si4+ (0.26Å). The polyhedral volume of the $REEO_8$ dodecahedron is correspondingly larger than the analogous ZrO_8 dodecahedron in zircon. Boatner (2002) reviews the structures, chemistry and physical properties of zircon-group REE phosphates in more detail. Due to the lanthanide contraction (ionic radii of light lanthanides are larger than those of heavy lanthanides) orthophosphates of light lanthanides, La through Gd, crystallize with the monoclinic monazite structure (Ni et al. 1995), which is described in the section on related structures.

791

Table 4. Chemical analyses of zircon from AGS

Samp. No	1	2	3	4	5	6	7	8	9	10	average
SiO2	32.17	32.27	30.86	32.43	32.47	32.29	32.17	32.21	32.34	32.05	32.13
ZrO2	65.27	65.03	61.81	65.29	65.24	64.96	65.1	64.99	65.29	65.24	64.8
HfO2	1.48	1.5	1.68	1.48	1.48	1.53	1.54	1.54	1.59	1.46	1.53
Th	352	352	791	176	352	264	264	352	nd	264	316
U	440	881	705	264	969	441	705	529	1058	881	687
Al	Nd	53	529	Nd	nd	106	53	nd	53	Nd	79
Sc	Nd	Nd	nd	Nd	nd	nd	nd	nd	nd	Nd	Nd
Y	2047	1259	2127	1811	1811	2126	2205	2205	1654	394	2764
Ce	85	Nd	nd	256	427	598	nd	nd	nd	256	162
Nd	86	257	nd	343	171	171	nd	86	nd	429	154
Sm	Nd	86	nd	Nd	86	172	172	259	172	Nd	95
Gd	Nd	Nd	1301	607	174	694	87	87	nd	174	312
Dy	Nd	871	1394	174	958	261	87	523	609	Nd	488
Yb	702.	1054	1756	1054	878	790	1229	1054	878	527	992.
Ca	71	71	429	71	71	71	71	nd	143	71	107
Fe	2254	4897	15390	1477	1166	777	622	777	1399	622	2938
Pb	Nd	346	87	87	346	260	nd	nd	nd	606	173
P	Nd	Nd	144.0	Nd	nd	nd	nd	nd	nd	Nd	-
∑REE	8734	2269	4452	2434	2695	2687	1576	2008	1661	1385	2204

nd = not detected All values in ppm except for SiO_2, ZrO_2, HfO_2 in Wt %

Table 5. Chemical analyses of zircon from AGL

Samp.No	1	2	3	4	5	6	7	8	9	10	average
SiO_2	32.3	32.0	32.5	32.2	32.4	31.9	32.0	32.1	32.5	32.4	32.2
ZrO_2	64.9	64.6	64.2	64.1	64.9	64.1	65.3	64.7	64.6	64.3	64.6
HfO_2	0.9	0.9	0.9	0.9	1.3	1.2	1.6	1.3	1.6	1.7	1.2
Th	264	176	352	264	264	nd	176	264	264	88	211
U	441	176	705	705	88	176	nd	176	705	705	388
Al	Nd	nd	318	nd	nd	nd	nd	nd	nd	Nd	32
Sc	Nd	65	65	65	130	65	65	nd	65	65	59
Y	2677	1811	1811	2914	nd	1654	nd	nd	nd	Nd	1087
Ce	171	171	1025	85	nd	nd	nd	171	85	Nd	171
Nd	172	nd	257	257	257	nd	343	nd	nd	429	172
Sm	431	nd	173	259	nd	nd	nd	86	nd	259	121
Gd	Nd	nd	nd	521	nd	nd	nd	1734	174	260	113
Dy	174	349	609	523	nd	174	87	nd	nd	609	253
Yb	966	1054	527	1054	527	790	88	88	351	264	571
Ca	72	nd	286	nd	72	143	143	72	214	143	114
Fe	1011	544	1788	777	389	311	1555	855	2798	699	1073
Pb	173	nd	259	347	nd	347	1732	953	nd	Nd	381
P	Nd	nd	97	113	nd	nd	nd	nd	nd	Nd	-
∑REE	1914	1573	2591	2699	784	965	518	518	610	1821	1399

nd = not detected All values in ppm except for SiO_2, ZrO_2, HfO_2 in Wt %

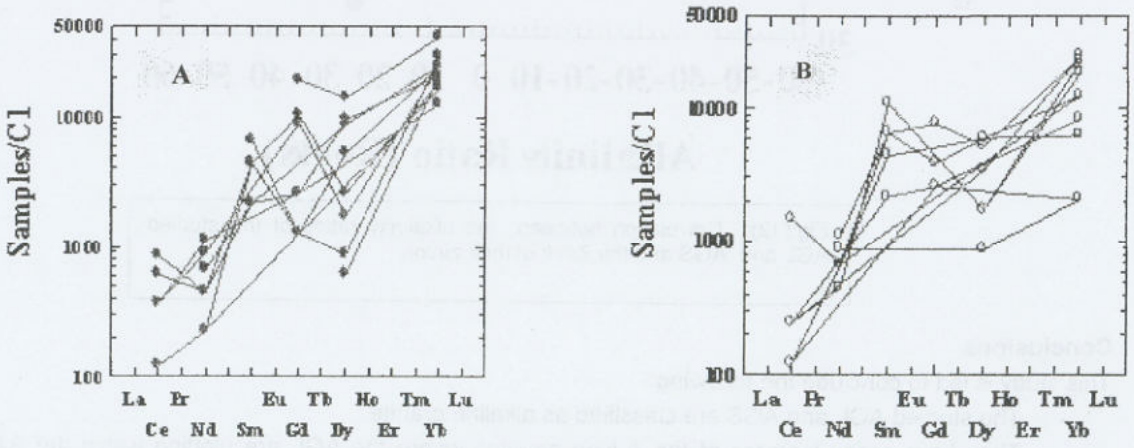

Fig. (11): Chondrite (CI) normalized (after Anders and Grevesse, 1989) REE patterns of different zircons from granitic rocks. A = zircons from AGS B = zircon from AGL

An attempt will be made to correlate between the alkalinity ratio on both AGL and AGS on one hand and the Zr/Hf ratios on zircon of the two rock units on the other hand. The calculated ratios are presented in table-6 and graphically represented as shown in figure 12. The figure shows that the Zr/Hf ratios of the studied zircons on both AGL and AGS are gradually increasing with their alkalinity ratios except for one sample of the AGS. This result is consistence with that obtained at figure 8A &B where the samples of the two rock units plot toward the alkalinity apex of the diagram.

Table (6): Alkalinity ratio and Zr/Hf of both AGL and AGS of the studied areas.

	Sample No.	43	33	45	8	94	28	D-7	D-8
AGL	Akal. Ratio	7.9	-23.46	9.27	13.64	12.32	9.76	-59. 6	57.9
	Zr/Hf	62.9	62.7	62.3	62.2	43.6	46.6	35.6	43.4
AGS	Sample No.	1	2	3	4	5	6	7	8
	Akal. Ratio	9.5	-19.9	24.9	11.1	-25.6	23	-39.7	20.39
	Zr/Hf	38.5	37.8	32.1	38.5	39.1	36.9	36.89	36.8

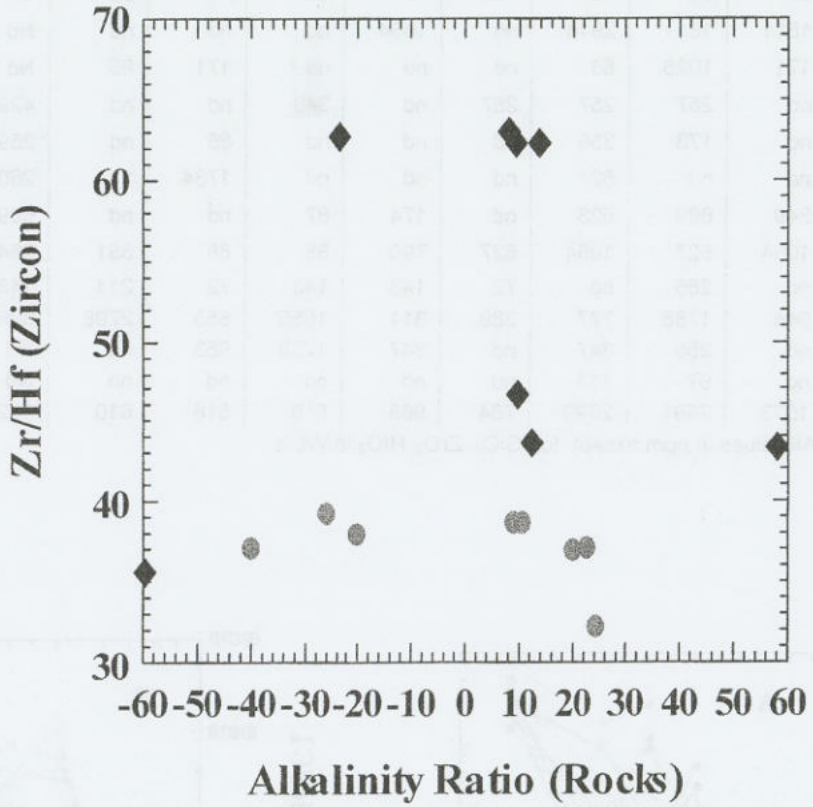

Fig.(12): Correlation between the alkalinity ratios of the studied AGL and AGS and the Zr/Hf of their zircon.

Conclusions

This study is led to conclude the following:

- The studied AGL and AGS are classified as alkaline granite.
- They have many features of the A-type granites where the AGL are plotting within the A1 field of Eby, 1992 while the AGS are considered as A2
- The two granitic plutons are crystallized in within-plate environment. Furthermore, the AGL have been emplaced at relatively deeper depth compared with the AGS which emplaced at shallow levels.
- The morphology of zircons were affected by the magma affinities, reflecting in development of pyramidal {101} feces.
- No direct correlation exists between the whole-rock REE and REE of zircon, the same conclusions were reached by Hoskin and Ireland (2000). Only the REE content of zircon may be affected by the concentration of P in the magma.
- The HfO_2 value of zircon has no significant for magma type.

- No distinct relation exists between whole-rock U & Th and U & Th contents of zircon. This can be attributed to changing in the uranium and thorium contents of the whole rock due to the post magmatic processes. Consequently, gain (in case of AGL) or loss (in case of AGS) of the two radioelements may be occurred. Controversially, the uranium and thorium incorporated in zircon are hardly affected by post magmatic processes. So no distinct relation can be observed between whole-rock U & Th and U & Th contents of zircon

References

1. Anders, E. and Grevesse, N. (1990): Abundances of the elements: Meteoritic and solar: Geochimica et Cosmochimica Acta, v. 53, p. 197-214.
2. Ballard, J. R., Palin, J. M. and Campbell, I. H. (2002): Relative oxidation states of magmas inferred from Ce(IV)/Ce(III) in zircon: application to porphyry copper deposits of northern Chile. Contributions to Mineralogy and Petrology 144 (3), 347– 364.
3. Barbey, P., Alle, P., Brouand, M. and Albarede, F. (1995): Rare-earth patterns in zircons from the Manaslu Granite and Tibetan slab migmatites (Himalaya)-insights in the origin and evolution of a crustally-derived granite magma. Chemical Geology 125 (1-2), 1-17.
4. Bea, F. (1996): Residence of REE, Y, Th and U in granites and crustal protoliths; implications for the chemistry of crustal melts. Journal of Petrology 37 (3), 521–552.
5. Belousova, E. A., Griffin, W. L. and Pearson, N. J. (1998): Trace element composition and cathodoluminescence properties of southern African kimberlitic zircons. Mineralogical Magazine, 62, 355–366.
6. Benisek, A. and Finger, F. (1993): Factors controlling the development of prism faces in granite zircons: a microprobe study. Contribution to Mineralogy and Petrology, 114, 441–451.
7. Boatner, L. A. (2002): Synthesis, structure, and properties of monazite, pretulite, and xenotime. Rev Mineral Geochem.48:87-121
8. Cherniak, D. J. and Watson, E. B. (2002): Pb diffusion in zircon. Chemical Geology,172. 25-41.
9. Condie, K. C. (1973): Aechean magmatism and crustal thickening. Geol. Soc. Am. Bull., 84, pp. 189-200.
10. De La Roche, H., Leterrier, J, Grand Cloude, P. and Marchal, M. (1980): A classification of volcanic and plutonic rocks using R1-R2 diagrams and major elements analysis, its relationships with current nomenclature. Chem. Geol., 183-210 pp.
11. Dickinson, J. E. Jr. and Hess, P. C. (1982): Zircon saturation in lunar basalts and granites. Earth Planet Sci Lett 57:336-344.
12. Eby, G. N. (1992): Chemical subdivision of the A-type granitoids: petrogenetic and tectonic implications. Geol., 20, pp. 641-644.
13. Fujimaki, H. (1986): Partition coefficients of Hf, Zr, and REE between zircon, apatite, and liquid. Contrib. Mineral Petrol. 94:42-45.
14. Gabr, M. M. (2005): Zircon typology and uranium mineralization of some younger granite plutons, south western Sinai, Egypt. Ph. D. Thesis, Suez Canal University, Egypt. 156pp (unpublished).
15. Geisler T., Schaltegger U. and Tomaschek, F. (2007): Re-equilibration of zircon in aqueous fluids and melts. Elements 3: 43-50.
16. Gromet, L. P. and Silver, L. T. (1983): Rare earth element distributions among minerals in a granodiorite and their petrogenetic implications. Geochim. Cosmochim. Act., vol. 47, p. 925- 939.
17. Halden, N. M., Hawthorne, F. C., Campbell, J. L., Teesdale, W. J., Maxwell, J. A., and Higuchi, D. (1993): Chemical characterization of oscillatory zoning and overgrowths in zircon using 3 MeV μ-PIXE. Can. Min., 31, 637–647.
18. Hanchar, J. M. and Miller C. F. (1993): Zircon zonation patterns as revealed by cathodoluminescence and backscattered electron images: implications for interpretation of complex crustal histories. Chem Geol 110:1-13.
19. Hanchar, J. M. and van Westrenen, W. (2007): Rare earth element behavior in zircon–melt systems. Elements 3: 37-42
20. Harley, S. L., Kelly, N. M. and Möller, A. (2007): Zircon behaviour and the thermal histories of mountain chains. Elements 3: 25-30
21. Heaman, L. M., Bowins, R. and Crocket, J. (1990): The chemical composition of igneous zircon suites: Implications for geochemical tracer studies: Geochimica et Cosmochimica Acta, v. 54, p. 1597–1607.
22. Hinton, R. W. and Upton, B. G. J. (1991): The chemistry of zircon-variations within and between large crystals from syenite and alkali basalt xenoliths. Geochimica et Cosmochimica Acta 55 (11), 3287–3302.
23. Hoffmann, C. (1981): Chi-square testing of zircon populations from an Archean granite-greenstone terrain, Minas Gerais, Brazil. Neues Jahrb Min. Abh., 140, 202–220.
24. Hoskin, P. W. O. and Ireland, T. R. (2000): Rare earth element chemistry of zircon and its use as a provenance indicator: Geology, v. 28, p. 627-630.
25. Hoskin, P. W. O. and Rodgers, K. A. (1996): Raman spectral shift in the isomorphous series (Zr1-xHfx)SiO4. Eur J Sol State Inorg Chem 33:1111-1121
26. Ireland, T. R. and Wlotzka, F. (1992): The oldest zircons in the solar system. Earth Planet. Sci. Lett. 109, 1–10.

27. KÖhler, H. (1970): Die änderung der Zirkonmorphologie mit dem differentiationsgrad eines Granits. Neues Jahrb Mineral Mh 9:405-420
28. Kostov, I. (1973): Zircon morphology as a crystallogenetic indicator. Krist. Tech., 8, 11-19.
29. Larsen, L. H. and Poldervaart, A. (1957): Measurement and distribution of zircons in some granitic rocks of magmatic origin. Min. Mag., 31, 544–564.
30. Mosalhi, M. (2006): Geological and radioactive studies on the granitoid rocks, north Ras Mohamed area, south Sinai, Egypt. Ph. D. Thesis, Suez Canal University, Egypt. 197pp (unpublished).
31. Nagasawa, H. (1970): Rare earth concentrations in zircon and their host dacites and granites. Earth Planet Sci Lett 9:359-364 Ni et al. 1995)
32. Ni, Y., Hughes, J. M. and Mariano, A. N. (1995): Crystal chemistry of the monazite and xenotime structures. Am Mineral 80:21-26
33. Paterson, B. A., Rogers, G. and Stephens, W. E. (1992): Evidence for inherited Sm-Nd isotopes in granitoid zircons. Contrib Mineral Petrol 111:378-390
34. Pearce, J. A., Harris, N. B. W. and Tindle, A. G. (1984): Trace element discrimination diagrams for the tectonic interpretation of granitic rocks. J. Petrol. 25 (4) 956 -983.
35. Poldervaart, A. (1955): Zircons in rocks, 1. Sedimentary rocks. Am. J. Sci., 253, 433–461.
36. Poldervaart, A. (1956): Zircon in rocks. 2. Igneous rocks. Am, J. Sci., 254, 521–554.
37. Poller, U., Huth J., Hoppe, P. and Williams, I. S. (2001): REE, U, Th, and Hf distribution in zircon from western Carpathian Variscan granitoids: a combined cathodoluminescence and ion microprobe study. Am J Sci 301:858-876
38. Pupin, J. P. (1980): Zircon and granite petrology. Contrib. Min. Petrol., 73, 207–220.
39.
40. Pupin, J. P. and Turco, G. (1972a): Une typologie originale du zircon accessoire. Bull Soc Fr Minéral Cristallogr., 95, 348–359.
41. Pupin, J. P. and Turco, G. (1972b): Application des données morphologiques du zircon accessoire en pétrologie endogène. C R Acad. Sci., 275D, 799–802. Paris.
42. Pupin, J. P. and Turco, G. (1972c): Le zircon accessoire en géothermométrie. C R Acad Sci, 274D, 2121–2124; Paris.
43. Ramakrishnan, SS., Gokhale, KVGK. And Subbarao, EC. (1969): Solid solubility in the system zircon-hafnon. Mater Res Bull 4:323-328.
44. Sawka WN (1988) REE and trace element variation in accessory minerals and hornblende from the strongly zoned McMurry Meadows Pluton, California. Trans Roy Soc Edinburgh: Earth Sci 79:157-168
45. Schaltegger, U., Fanning, CM., Günther, D., Maurin, JC., Schulmann, K. and Gebauer, D. (1999): Growth, annealing and recrystallization of zircon and preservation of monazite in high-grade metamorphism: conventional and in-situ U-Pb isotope, cathodoluminescence and microchemical evidence. Contrib Mineral Petrol 134:186-201.
46. Silver, LT. and Deutsch, S. (1963): Uranium-lead isotopic variations in zircons: a case study. J Geol 71:721-758.
47. Shimron, A.E., 1980. Proterozoic island arc volcanism and sedimentation in Sinai. Precambrian Research 12, 437–458.
48. Speer, JA. (1982): Zircon. Rev Mineral 5:67-112.
49. Uher, P., Breiter, K., Kleèka, M. and Pivec, E. (1998): Zircon in highly evolved Hercynian Homolka Granite, Moldanubian Zone, Czech Republic: indicator of magma source and petrogenesis. Geologica Carpathica 49:151-160.
50. Vavra, G. (1990): On the kinematics of zircon growth and its petrogenetic significance: a cathodoluminescence study. Contrib. Min. Petrol., 106, 90–99.
51. Vavra, G. (1993): A guide to quantitative morphology of accessory zircon. Chem. Geol., 110, 15–28.
52. Vavra, G. (1994): Systematics of internal zircon morphology in major Variscan granitoid types. Contrib Mineral Petrol 117:331-334.
53. Wang, X., Griffin, WL., O'Reilly, SY., Zhou, XM. Xu. XS., Jackson, SE. and Pearson, NJ. (2002): Morphology and geochemistry of zircons from late Mesozoic igneous complexes in coastal SE China: implicaitions for petrogenesis. Mineral Mag 66:235-251.
54.
55. Wark, DA. And Miller, CF. (1993): Accessory mineral behavior during differentiation of a granite suite: monazite, xenotime and zircon in the Sweetwater Wash pluton, southeastern California, U.S.A. Chem Geol 110:49-67.
56. Watson, EB. (1979): Zircon saturation in felsic liquids: experimental results and pplications to trace element geochemistry. Contrib Mineral Petrol 70:407-419.
57. Watson, EB. (1980): Some experimentally determined zircon/liquid partition coefficients for the rare earth elements. Geochim Cosmochim Acta 44:895-897.
58. Watson, EB. And Harrison, TM. (1983): Zircon saturation revisited: temperature and composition effects in a variety of crustal magma types. Earth Planet Sci Lett 64:295-304.
59. Whalen, J. B. Currie, K. I. and Chappell, B. W. (1987): A-type granites: geochemical characteristic, discrimination and petrology. Contrib. Min. Petrol., 95, 407-419.
60. Wopenka, B., Jolliff, BL., Zinner E. and Kremser, DT. (1996): Trace element zoning and incipient metamictization in a lunar zircon: application of three microprobe techniques. Am Mineral 81:902-912.